JMEPEG (1996) 5:335-352

Bulk Deformation of Ti-6.8Mo-4.5Fe-1.5Al (Timetal LCB*) Alloy

I. Weiss, R. Srinivasan, M. Saqib, N. Stefansson, A.G. Jackson, and S.R. LeClair

Recently, a low-cost near-β titanium alloy (Timetal LCB Ti-6.8Mo-4.5Fe-1.5Al wt%) containing iron and molybdenum has been developed. This alloy is cold formable in the β microstructure and can be aged to high strengths by precipitating the α phase. Due to its combination of cold formability and high strength, the alloy is a potential replacement for steel components in the automotive industry. The current study was undertaken to evaluate the cold bulk forming characteristics of Timetal LCB for use in lightweight automotive applications. Room-temperature compression tests conducted over a strain-rate range of 0.01 to 5/s indicate that the bulk cold compression of the alloy is affected by two factors: the microstructure and the length-to-diameter aspect ratio of the specimen. In the aged condition, when the microstructure has α-phase particles distributed along flow lines in the β-phase matrix, the alloy has the propensity for shear failure when deformed in compression in a direction parallel to the flow lines. In the solution-heat-treated condition, the microstructure consists of β grains with athermal ω phase. In this condition, the alloy can be cold compressed to 75% reduction in height using specimens with aspect ratio of 1.125, but fails by shear for a larger aspect ratio of 1.5. Plastic deformation of the material occurs initially by single slip in most grains, but changes to multiple slip at true plastic strains larger than about 0.15. At a slow strain rate, the deformation is uniform, and the material work hardens continuously. At high strain rates, shear bands develop, and the localized deformation and temperature rise due to deformation heating leads to flow softening during compression. Although there is a considerable rise in temperature (200 to 500 °C) during deformation, precipitation of the α phase was not observed.

Keywords

beta titanium alloys, compression testing, LCB titanium, shear bands, work hardening and softening

1. Introduction

TITANIUM alloys are of growing interest for automotive applications due to the requirements placed on automobile manufacturers to increase the fuel economy of cars. Titanium alloys have long been used in the aerospace industry because of their high specific strength and stiffness, where cost is a secondary issue in comparison to weight. Similarly, cost is secondary to performance in racing cars, and titanium alloys have been successfully used for springs and engine valves. In commercial automotive applications—passenger cars and light trucks—titanium alloys must compete with existing materials not only on the basis of weight or performance, but also on the basis of cost. Therefore, both material and processing costs must be minimized.

The introduction of a new material poses a number of questions and challenges. Can the material outperform currently used materials (i.e., steel)? Can this material be processed by the same methods currently used for steel? If not, what other processing options are available? Are these alternative methods cost effective, and will the parts made with the new material be affordable? The answer, in the case of titanium alloy components, is that they have the potential to perform better than steel components in many automotive applications, but are expensive in terms of material costs. The development of low-cost titanium alloys and processing technologies is important if titanium alloys are to be used extensively in the automotive industry.

The room-temperature structure of titanium alloys consists of all alpha phase (α hexagonal close-packed, or hcp, structure), or all beta phase (β body-centered cubic, or bcc, structure), or a mixture of alpha and beta phases (α + β). If the amount of elements such as vanadium and molybdenum, referred to as β-stabilizing elements, is greater than a critical amount, the structure at room temperature consists entirely of the β phase (Ref 1). Some alloys with β-stabilizing elements less than this critical amount can be cooled rapidly from above the α + β to β-transus temperature to retain a metastable structure of β phase at room temperature. These alloys are called the near-β alloys. Because the near-β alloys have a metastable microstructure, the strength of these alloys can be controlled through heat treatment and precipitation of the α phase (Ref 2). However, due to the microstructural instability of these alloys, their use is limited to below about 250 °C (480 °F) (Ref 3).

Recently, a new low-cost β-titanium alloy has been developed. Known as Timetal LCB (Ti-4.5Fe-6.8Mo-1.5Al, in weight percent), the alloy uses the β-stabilizing element molybdenum, added in the form of a ferro-moly compound. In the solution-heat-treated and quenched condition, the alloy has a β-phase (bcc) structure at room temperature. It thus possesses excellent workability compared to alloys containing the α phase (hcp). Aging the alloy at a temperature 30 to 100 °C (55 to 180 °F) below the transus temperature causes the α phase to precipitate. In this condition, the alloy has a yield strength greater than 900 MPa (130 ksi) and a tensile elongation of about 18% (Ref 4, 5), which compares favorably with high-strength steels.

*TIMET, Henderson, NV

I. Weiss, R. Srinivasan, M. Saqib, and **N. Stefansson,** Mechanical and Materials Engineering Department, Wright State University, Dayton, OH 45435, USA; **A.G. Jackson** and **S.R. LeClair,** Wright Laboratory—Materials Directorate, WL/MLIM, Wright-Patterson AFB, OH 45433, USA.

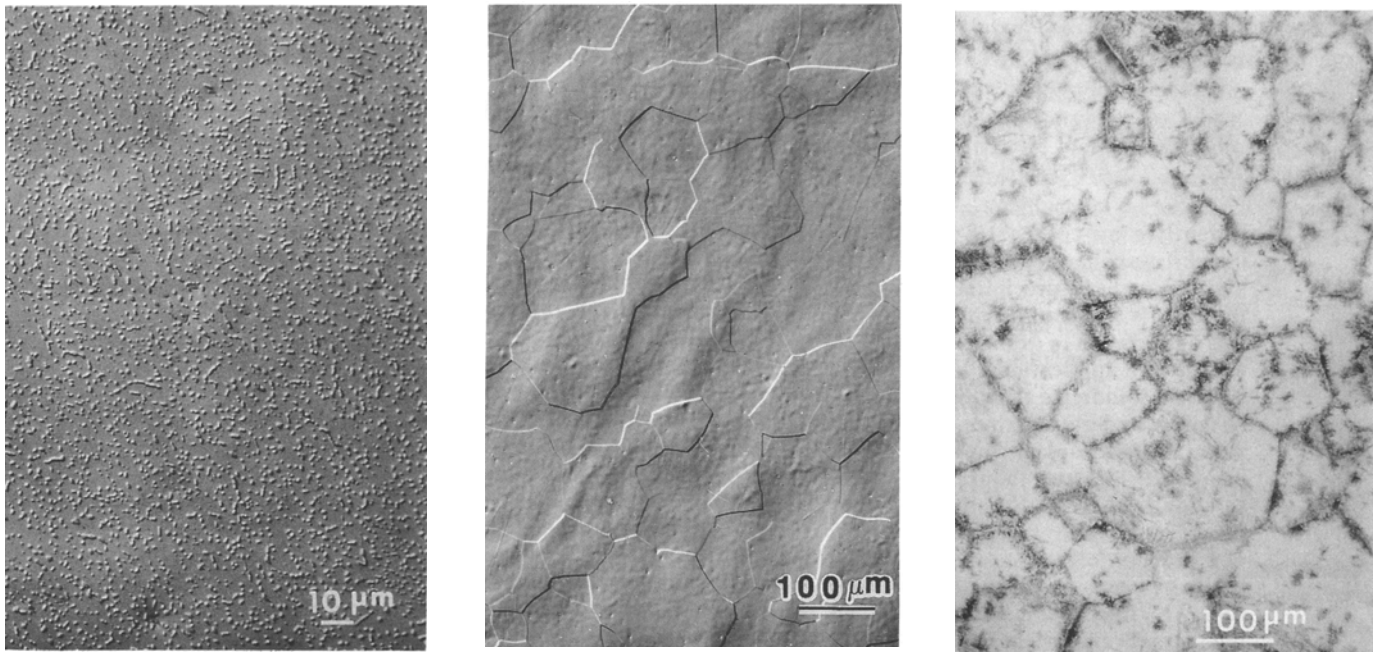

(a) (b) (c)

Fig. 1 Microstructure of Timetal LCB alloy. (a) As-received. (b) Solution heat treated at 815 °C (1500 °F) for 30 min and air cooled at 5 °C/s (9 °F/s). (c) Solution heat treated at 815 °C (1500 °F) and furnace cooled

This paper presents the results of a study of the cold deformation behavior of Timetal LCB titanium alloy. Compression tests were carried out at different strain rates over a temperature range of 25 to 290 °C (77 to 550 °F). Specimens of two length-to-diameter (aspect) ratios of 1.5 to 1.125 were used. Microstructural development during deformation was followed by interrupting tests at different strains. The purpose was to determine the effect of different processing parameters on the cold formability of this alloy.

2. Materials and Experimental Procedures

The as-received LCB titanium alloy had been hot rolled to a 50 mm (2 in.) diam bar and then aged at 790 °C (1450 °F) for 30 min, followed by air cooling. The microstructure of the as-received material, shown in Fig. 1(a), consists of fine α-phase particles in a β-phase matrix. The as-received material was then solution heat treated at 815 °C (1500 °F) for 30 min and air cooled at 5 °C/s (9 °F/s). This temperature is above the α + β-transus temperature of about 800 °C (1475 °F) for this alloy (Ref 4). This heat treatment yielded a microstructure consisting of β grains in the 50 to 200 μm size range (Fig. 1b). If the alloy is furnace cooled at a slow cooling rate, α-phase particles precipitate both within the β grains and along the prior-β grain boundaries (Fig. 1c) Rapid cooling is thus necessary to prevent α-phase precipitation and to retain the β phase at room temperature.

Specimens with a length-to-diameter (aspect) ratio of 1.5, measuring 10.2 mm (0.4 in.) diameter and 15.3 mm (0.6 in.) in height, were electrical discharge machined and surface ground. Samples of a smaller aspect ratio of 1.125 were also prepared in the same manner. All samples were then solution heat treated at 815 °C (1500 °F) and air cooled at 5 °C/s (9 °F/s).

Compression tests were carried out on an MTS (MTS Systems Corp., Eden Prairie, MN) hydraulic testing system, controlled by the MTS TestStar (MTS Systems Corp., Eden Prairie, MN) system. Constant-strain-rate compression tests were carried out at strain rates of 0.01, 0.1, 1, and 5/s at 25, 150, 205, and 290 °C (77, 300, 400, and 550 °F). A graphite-base lubricant, DeltaForge 31, (Acheson Colloids Co., Port Huron, MI) was used between the specimen and die surfaces to minimize the effect of friction. Data were recorded in the form of load and ram displacement as a function of time. These data were then converted to nominal true stress/true strain flow curves.

3. Results

3.1 *Macroscopic Deformation*

Samples of LCB titanium alloy (β-transus temperature ≈ 800 °C, or 1470 °F) with an aspect ratio of 1.5 were compressed to 50% reduction in height (true strain of about 0.7) at room temperature (25 °C, or 77 °F) at strain rates between 0.01 and 5/s. At all the strain rates tested, samples failed by shear cracking, as shown in Fig. 2. The initiation of shear failure occurred as soon as the deformation was imposed on the specimens. This was true for both the as-received material, which had been aged at 790 °C (1450 °F) (subtransus), and material that had been solution heat treated at 815 °C (1500 °F) (supertransus) and air cooled.

Samples with a lower aspect ratio of 1.125 were then deformed under the same conditions. Material that had been heat treated at 815 °C (1500 °F) deformed with no macroscopically observable cracking to a reduction in height of 75% (true strain

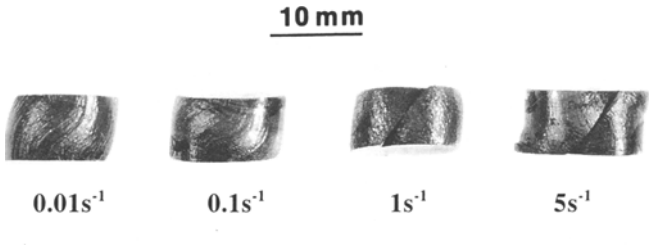

Fig. 2 Shear failure of samples with length-to-diameter aspect ratio of 1.5, solution heat treated at 815 °C (1500 °F) for 30 min, air cooled at 5 °C/s (9 °F/s), and deformed at room temperature to 50% reduction in height, at different strain rates

of 1.4) at strain rates up to 5/s, as shown in Fig. 3. However, samples of the as-received material, with a subtransus heat treatment at 790 °C (1450 °F), failed even when the smaller aspect ratio of 1.125 was used. These results confirm that the subtransus annealing, which causes α-phase precipitation, also greatly increases the flow stress and reduces the ductility of the alloy. Subsequent compression tests were all carried out on material that had been solution heat treated at 815 °C (1500 °F) and cooled at 5 °C/s (9 °F/s) to room temperature.

3.2 *Flow Curves at Room Temperature*

Figure 4 presents flow curves for the deformation of LCB titanium at room temperature, to approximately 75% reduction in height, showing the variation of the average true stress ($\sigma = P/A$) with nominal true strain ($\varepsilon = \ln[h_0/h]$). Although the yield stress of the alloy increases with increasing strain rate, deformation at high strain rates of 1 and 5/s results in flow softening following yielding. At slower strain rates of 0.01 and 0.1/s, the flow curves show work hardening.

Figure 5 shows the effect of strain rate on yield stress at room temperature. The yield stress varies between 1025 and 1250 MPa (150 and 180 ksi) for strain rates in the range of 0.01 to 5/s (Fig. 5a). The strain-rate-sensitivity parameter (slope of the $\log(\sigma)$ versus $\log(\dot{\varepsilon})$ curve) is about 0.03 (Fig. 5b). At strains larger than about 0.2, there is an inverse dependence of flow stress on strain rate, probably due to deformation heating and deformation localization. The temperature rise during a compression test was estimated assuming that 95% of the work of deformation was converted to heat, with a fraction of the heat being retained to uniformly heat the specimen (Ref 6). As seen in Fig. 6, the temperature rise at strain rates greater than 1/s can be almost 500 °C (900 °F).

3.3 *Flow Curves for Warm Deformation*

Since considerable deformation heating occurs in specimens that are initially at room temperature, additional compression tests were carried out at 150, 205, and 290 °C (300, 400, and 550 °F). Figures 7(a) and 8(a) show flow curves for compression tests carried out at strain rates of 1 and 5/s, respectively. The yield stress at both strain rates decreases as temperature increases, as shown in Fig. 9.

At a strain rate of 1/s, there is continuous flow softening at room temperature. As the initial deformation temperature is raised, however, there is a decrease in the flow stress level, as well as a change in the work-hardening behavior. The flow

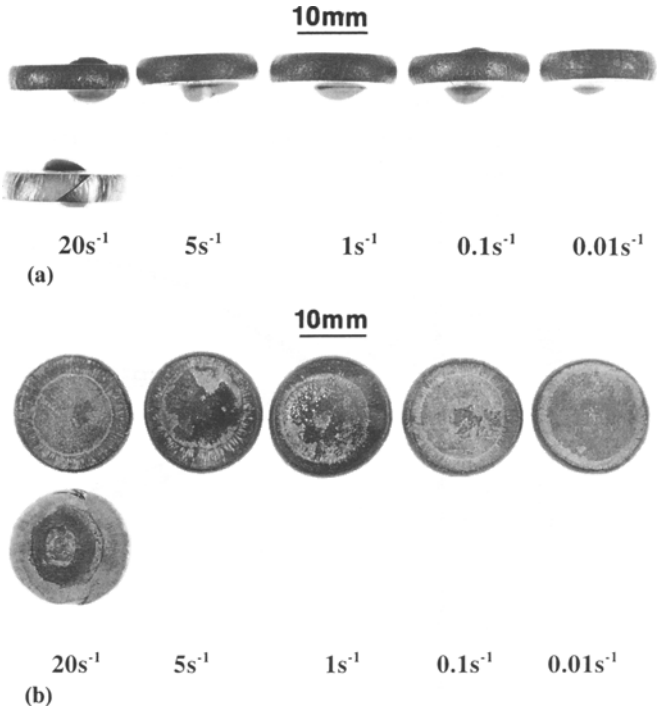

Fig. 3 Shape of LCB titanium samples with length-to-diameter aspect ratio of 1.125 deformed by compression to 75% reduction in height at the indicated strain rates. The first row of samples in both (a) and (b) were solution heat treated at 815 °C (1500 °F) for 30 min and air cooled at 5 °C/s (9 °F/s), and the sample in the second row was in the as-received condition. (a) Side view. (b) Top view

curve at 150 °C (300 °F) shows a distinct yield point followed by almost constant flow stress, whereas at 205 °C (400 °F) there is a small amount of work hardening followed by deformation, with little change in flow stress. At 290 °C (550 °F), however, there is continuous work hardening. Figure 7(b) shows that at a strain rate of 1/s, even when the initial test temperature is increased, the estimated temperature rise can be in the range of 350 to 500 °C (660 to 930 °F) for deformation to a strain of 1.3.

Figures 8(a) and (b) show the flow stress and estimated average temperature rise in specimens deformed at a strain rate of 5/s. At this strain rate, considerable flow softening occurs, even at an initial temperature of 150 °C (300 °F). Upon increasing the temperature to 205 °C (400 °F), there is a distinct yield point, followed by work hardening up to a strain of 0.35, beyond which the material work softens. Again, the estimated temperature increase is in the range of 350 to 500 °C (660 to 930 °F).

4. Discussion

4.1 *Instability during Compressive Deformation*

Compressive deformation of a work-hardening material is inherently stable; that is, the load required to cause deformation increases with increasing strain, since both the cross-sectional area and the flow stress increase with strain. This holds true as long as deformation remains uniform. Plastic instability and nonuniform deformation can occur during compression because

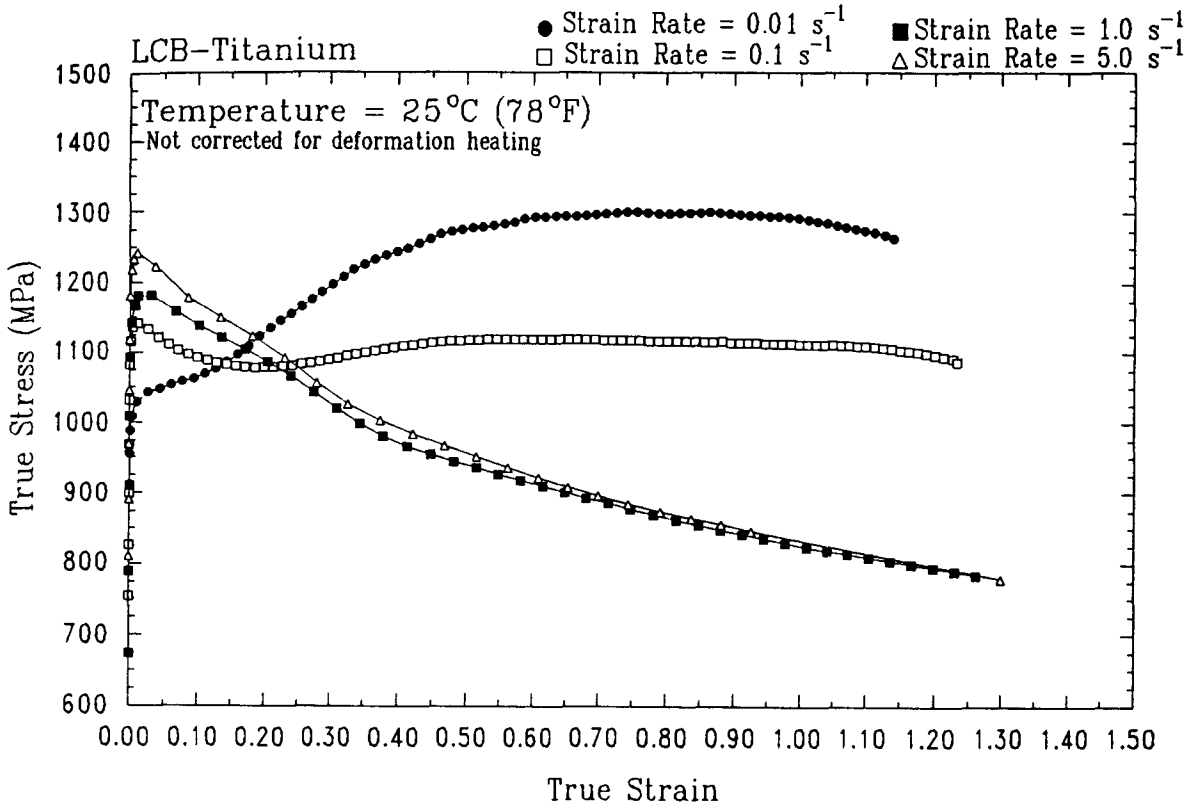

Fig. 4 Nominal true stress/true strain curves for the LCB alloy deformed at room temperature

of friction at the specimen die interfaces, the height-to-diameter aspect ratio of the specimen, and flow softening of the materials due to recovery or recrystallization. Because recovery and recrystallization generally occur at elevated temperature, they usually do not contribute to flow softening at room temperature.

Friction at the specimen die interface results in the formation of dead metal zones, with little or no deformation near the die contact surfaces and bands of light shear deformation just outside the dead metal zones (Ref 7). Subsequent deformation could be confined to the shear bands. If the room-temperature flow stress of a material is very high, but decreases significantly with increasing temperature, deformation heating can soften the material in the bands, resulting in further localization (Ref 8). This type of adiabatic shear failure has been observed in $\alpha + \beta$ Ti-6Al-4V titanium alloy at high deformation rates. However, at slow strain rates, when quasi-static deformation conditions prevail, nearly uniform deformation occurs without the formation of shear bands (Ref 9).

The effect of friction can be reduced by increasing the height-to-diameter aspect ratio of the specimens. However, if the aspect ratio becomes too large, the specimen may buckle. During compression testing, aspect ratios in the range of 1.5 to 2 are used to strike a balance between the tendency of a specimen to buckle and the effects of friction.

The as-received LCB material had been hot rolled in the β phase and then given a final aging treatment at 790 °C (1450 °F). This resulted in the precipitation of α particles along flow lines in the β-phase matrix, and a distinct morphological texture, which can be seen in both the macro- and microstructure as bands in the axial direction (Fig. 10). Such a microstructure has the propensity to adiabatic shear failure, especially in titanium alloys (Ref 9). It is thus not surprising that specimens of the as-received material, with both high and low aspect ratios of 1.5 and 1.125, respectively, failed by adiabatic shear.

When the LCB alloy is solution heat treated above the β-transus temperature and rapidly cooled to room temperature, there is very little α phase in the microstructure. However, the material is still textured and, due to its work-hardening behavior, continues to be susceptible to shear failure. These issues are discussed in subsequent sections.

4.2 *Work-Hardening Behavior*

A material that exhibits work hardening shows a positive work-hardening rate ($\delta\sigma/\delta\varepsilon$), but this rate decreases with increasing strain. A work-softening material has a negative work-hardening rate, and, for many metals, the rate of softening also decreases with increasing strain. When a material exhibits a yield point, the work-hardening rate is negative; that is, flow softening occurs immediately after yielding. In metals such as low-carbon steels, work hardening can occur after the yield point. Thus, depending on the type of mechanism controlling the deformation, the work-hardening behavior may be different. For dual-phase steels, different work-hardening behaviors have been observed at low strains. The observed behavior can be related to microstructural changes, specifically the martensite volume fraction resulting from thermomechanical processing (Ref 10).

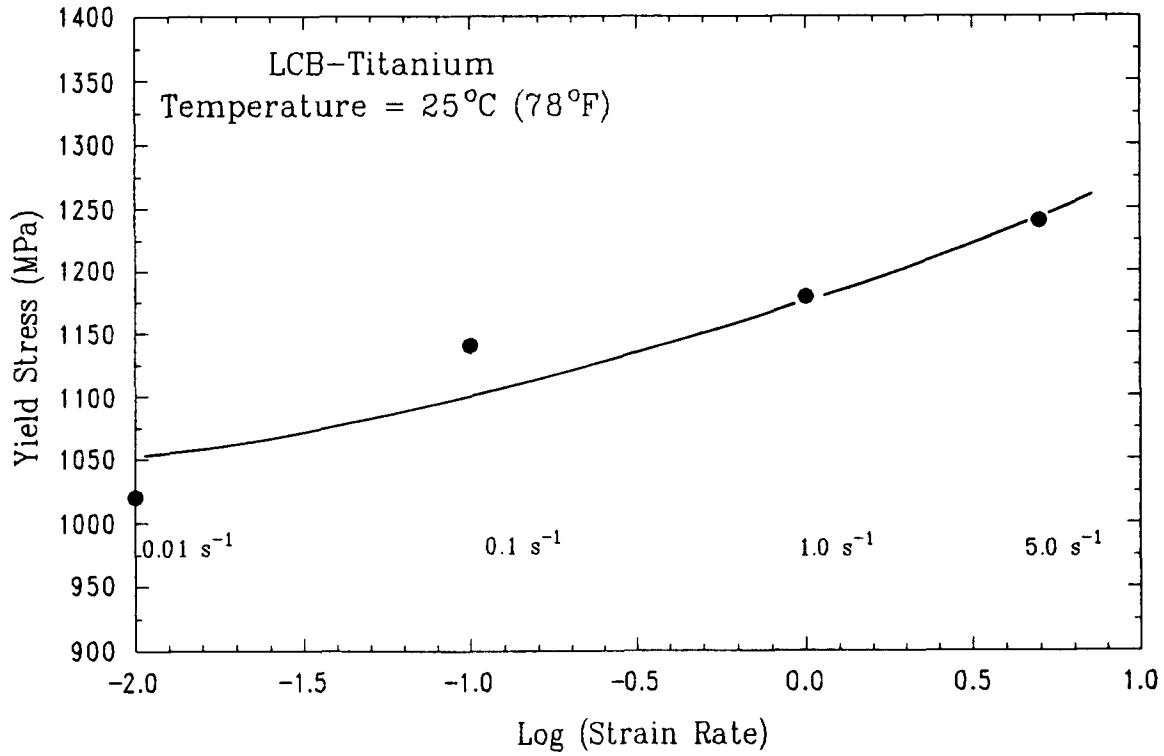

(a)

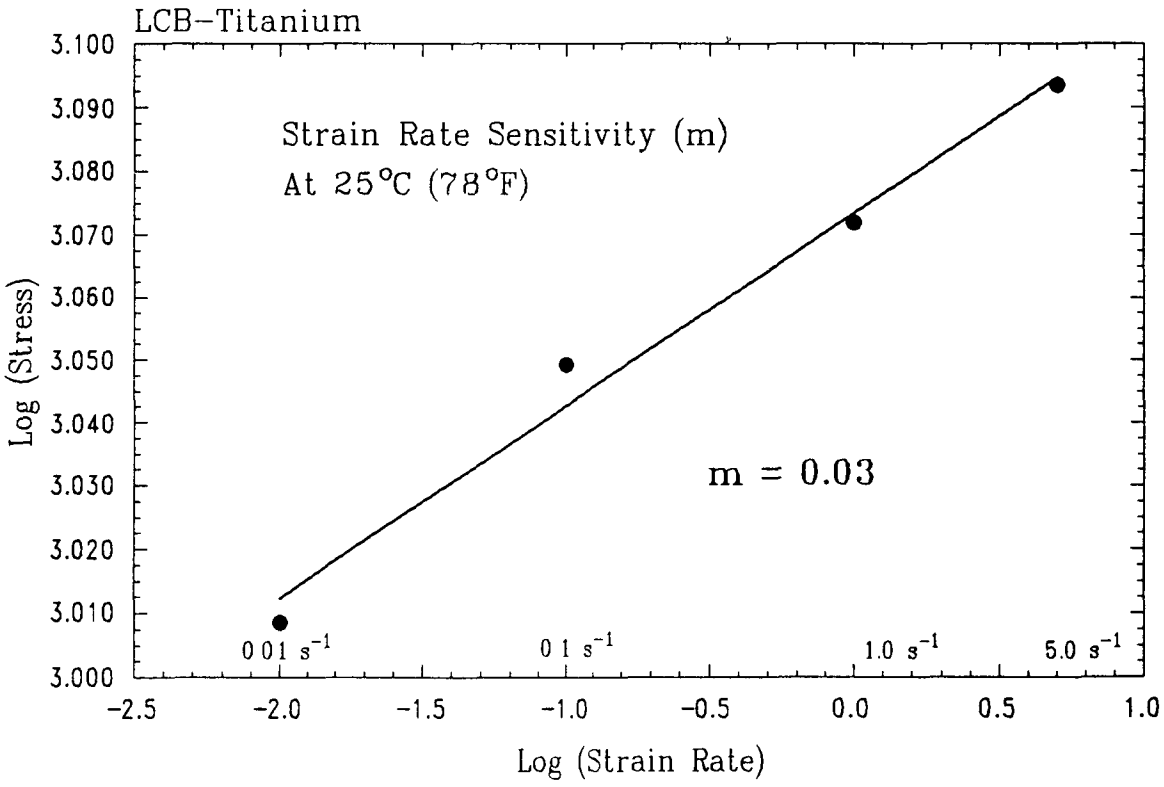

(b)

Fig. 5 Variation of yield stress with strain rate during room-temperature compression of the LCB alloy. (a) Yield stress (σ) as a function of log ($\dot{\epsilon}$). (b) Log (σ) as a function of log ($\dot{\epsilon}$)

Figure 11 shows the normalized work-hardening parameter, $\gamma = ([1/\sigma][\delta\sigma/\delta\varepsilon])$, for the LCB alloy as a function of plastic strain for different strain rates at room temperature. At a strain rate of 0.01/s, the work-hardening parameter following yielding is very high and then rapidly drops to a small positive value of about 0.25. There is apparently a change in the deformation mode at a strain of 0.06, after which the work-hardening parameter increases sharply to a maximum of 0.75 at a strain of about 0.18. At larger strains, γ decreases, becoming negative beyond a strain of about 0.9. However, there is a continuous increase in load during the entire deformation. Therefore, deformation at a strain rate of 0.01/s is stable. Figures 12 (a) to (c) are macrographs of specimens deformed to strains of 0.06, 0.18, and 1.15, respectively, at a strain rate of 0.01/s. No shear bands are observed in these specimens. However, at the large strain of 1.15, dead metal zones, formed due to friction at the die contact surfaces, can be seen.

At a strain rate of 0.1/s, there is a yield point, which is immediately followed by a decrease in flow stress—that is, work softening occurs ($\gamma < 0$). But the value of γ increases, and becomes positive, after a strain of approximately 0.18. Since the material work hardens, one can expect stable deformation at this strain rate.

At the fast strain rates of 1 and 5/s, γ is negative during the entire deformation. The normalized work-hardening parameter is initially as low as –0.75. However, as was observed for deformation at a strain rate of 0.1/s, the rate of softening decreases (γ becomes less negative). Had the work-hardening parameter become positive, stable deformation of the material would have occurred. However, instead of the work-hardening parameter increasing, it becomes more negative beyond a strain of about 0.15.

The initiation of a shear band during compressive deformation can be related to the ratio of the work-hardening parameter, γ, to the strain-rate-sensitivity parameter, m (Ref 11). Shear bands are initiated if the value of $(-\gamma/m)$ exceeds a critical value. This analysis is valid for both hot and cold deformation. The critical value of $(-\gamma/m)$ during hot deformation of several titanium alloys is about 5 (Ref 12). Figures 5(b) and 11 show that for cold deformation of the LCB titanium alloy, the value of m is only about 0.03, and γ is on the order of –0.5 at strain rates of 1 and 5/s up to a strain of 0.15. The ratio $(-\gamma/m)$, therefore, is greater than 15. It is thus plausible that the decrease in γ beyond a strain of 0.15 is the result of the formation of shear bands. Macrostructural examination of a specimen deformed to a strain of 0.26, where γ has the lowest value, indicates the presence of a shear band in the specimen (Fig. 13a). Once the shear band has been initiated, further deformation could become confined to the bands.

Due to the high stress levels and fast strain rates, a large amount of deformation heat is generated. Since the flow stress of the material decreases considerably with increasing temperature, as indicated in Fig. 7(a) and 8(a), the temperature rise could result in further localization of deformation within the shear band. However, beyond a strain of 0.26, γ begins to increase again, indicating a decreasing tendency toward deformation in the shear band. The increase in the value of γ is due to the spread of deformation away from the initial shear band. Figure 13(b) shows the spread of deformation away from the shear band, but the spread is limited by the formation of dead metal zones.

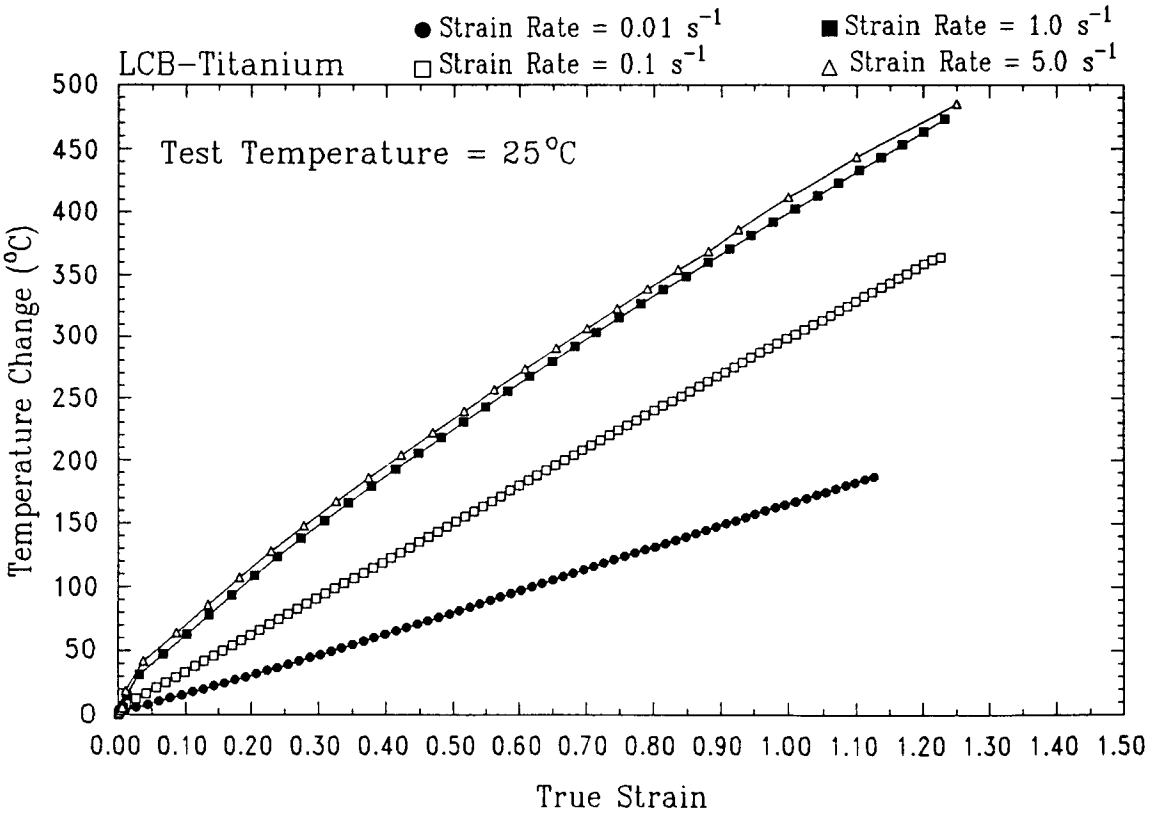

Fig. 6 Estimated temperature rise due to deformation heating for tests conducted at room temperature

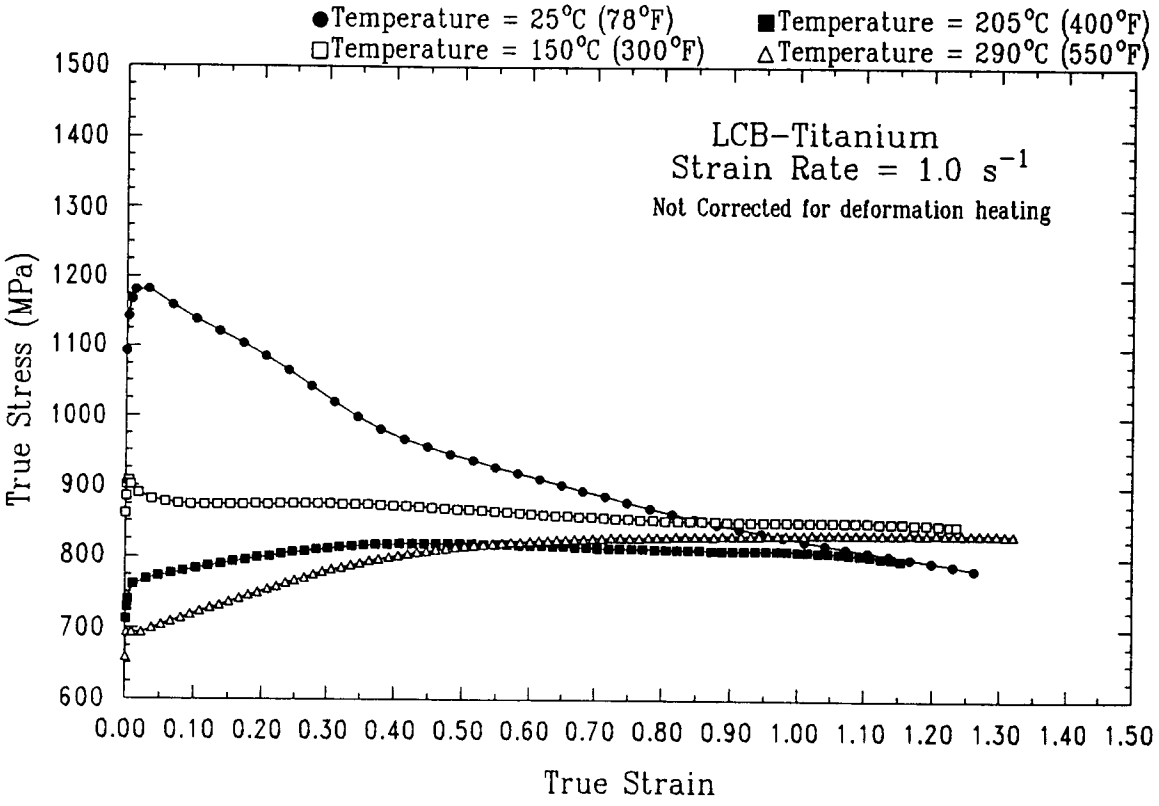

(a)

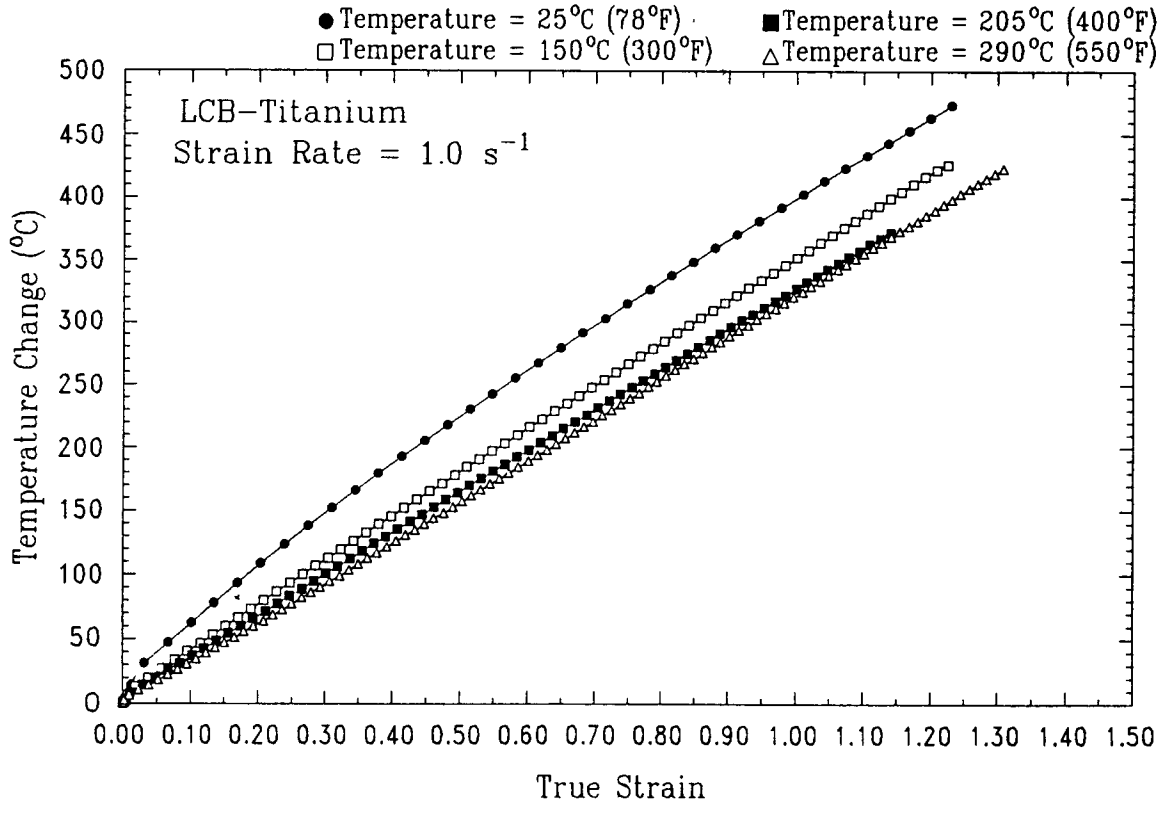

(b)

Fig. 7 (a) Flow curves for warm compression tests conducted at a strain rate of 1/s. (b) Estimated temperature rise of specimens due to deformation heating

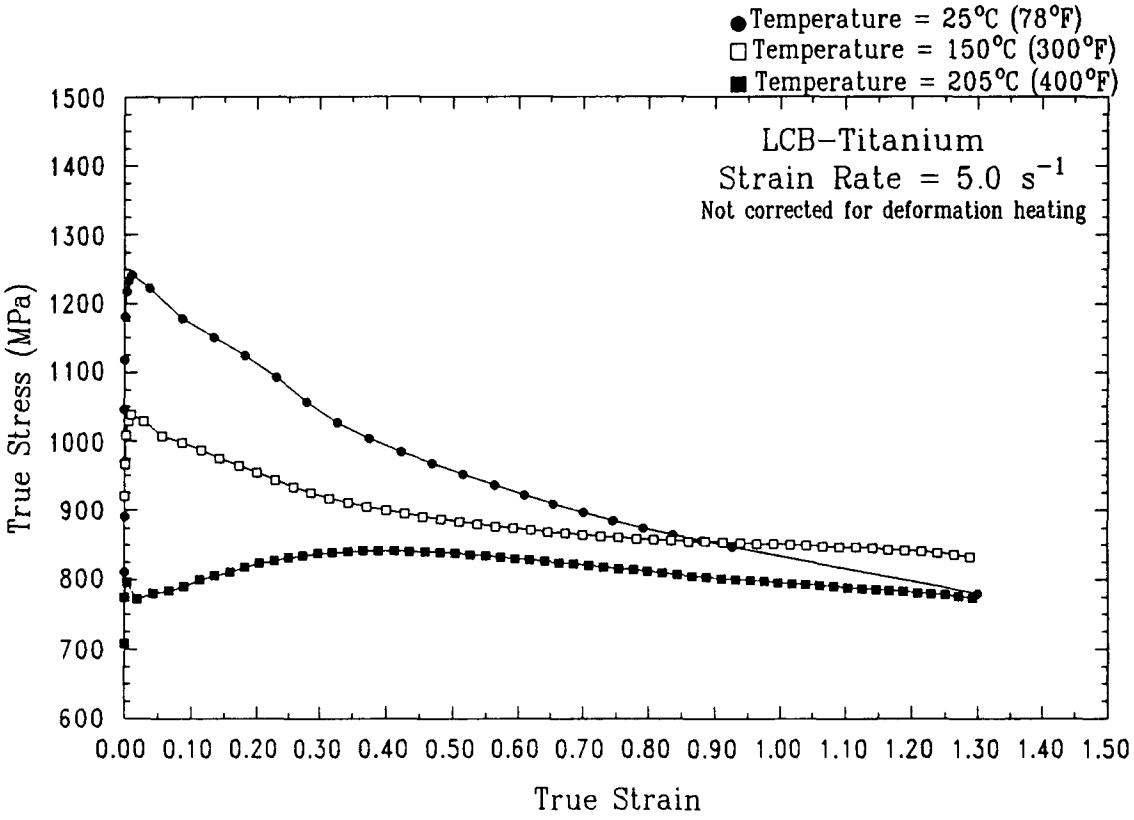

(a)

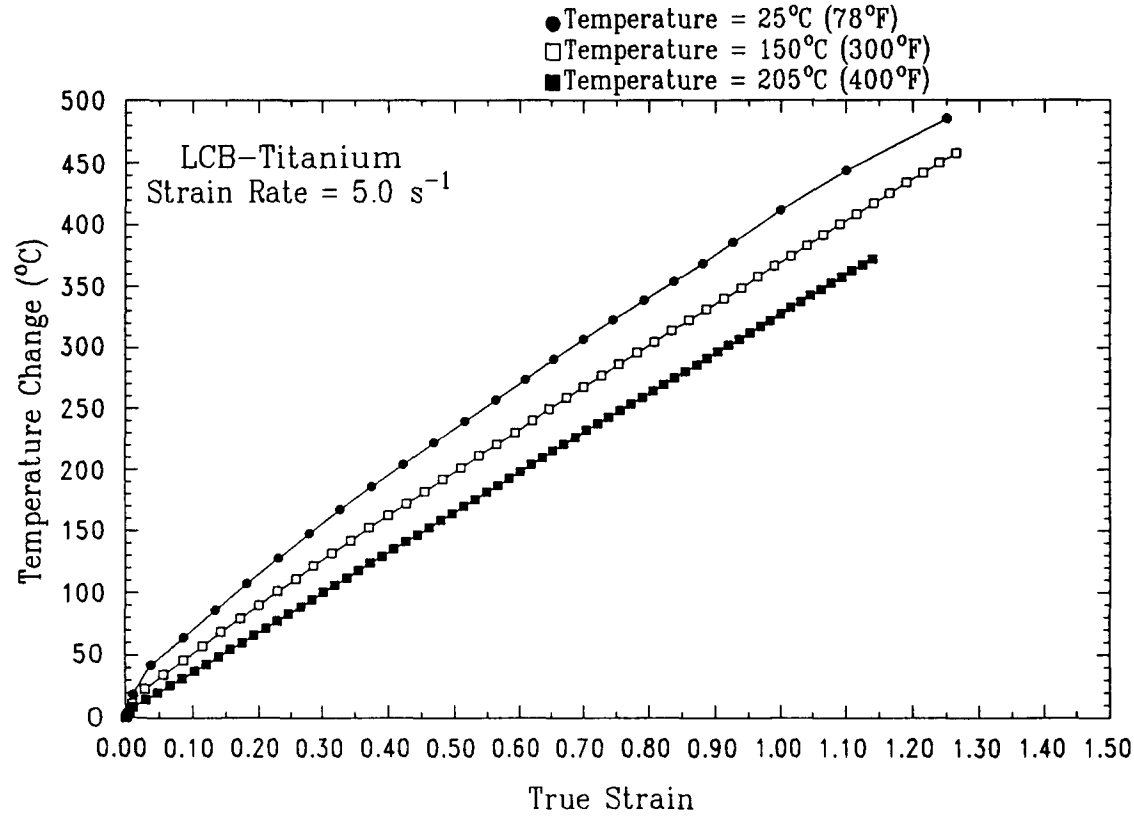

(b)

Fig. 8 (a) Flow curves for warm compression tests conducted at a strain rate of 5/s. (b) Estimated temperature rise of specimens due to deformation heating

Figures 14(a) and (b) show the variation in work-hardening behavior with strain at different temperatures and at strain rates of 1 and 5/s. At both strain rates, the material work softens at room temperature. At 150 °C (300 °F), initial work softening occurs. At a strain rate of 1/s, steady-state behavior ($\gamma = 0$) is observed beyond a strain of 0.15. Deformation at a faster strain rate of 5/s postpones steady-state behavior to a strain of 0.9. At 205 °C (400 °F), deformation at a strain rate of 1/s shows a positive work-hardening rate that decreases with increasing strain (Fig. 14a). The stress reaches a steady state beyond a strain of about 0.5 (Fig. 7a), which results in a zero work-hardening rate. Increasing strain rate to 5/s at 205 °C (400 °F) results in the appearance of a yield point. Subsequently, work-hardening behavior is similar to that at a strain rate of 1/s. At 290 °C (550 °F), however, the work-hardening rate at a strain rate of 1/s is higher than at 205 °C (400 °F), and flow stress value exceeds that for a specimen initially at 205 °C (400 °F) at strains greater than about 0.6 (Fig. 7a). This phenomenon may be related to the microstructural instability of the material above about 250 °C (480 °F) (Ref 3).

4.3 *Microstructural Changes during Cold Deformation*

4.3.1 The Starting Microstructure

The as-received material was annealed above the β-transus temperature at 815 °C (1500 °F) for about 30 min and rapidly cooled at 5 °C/s (9 °F/s) to room temperature. The resulting

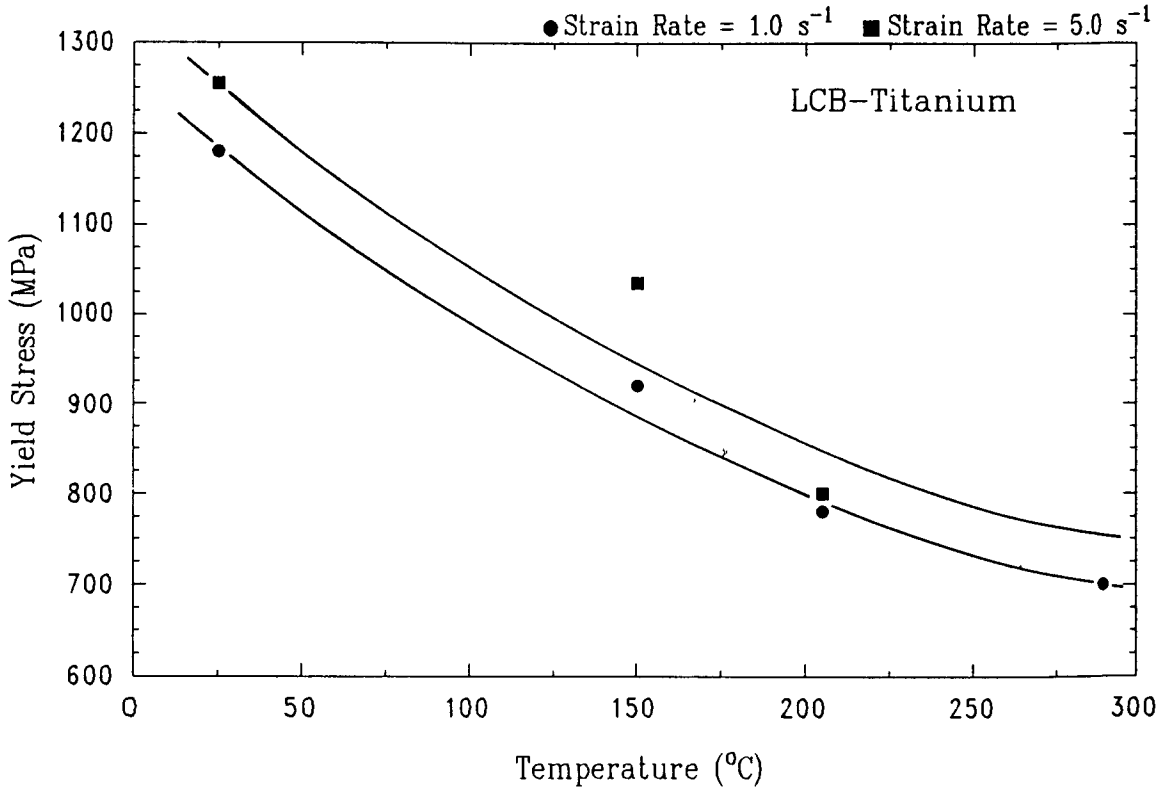

Fig. 9 Effect of temperature on yield stress for compression tests conducted at strain rates of 1 and 5/s

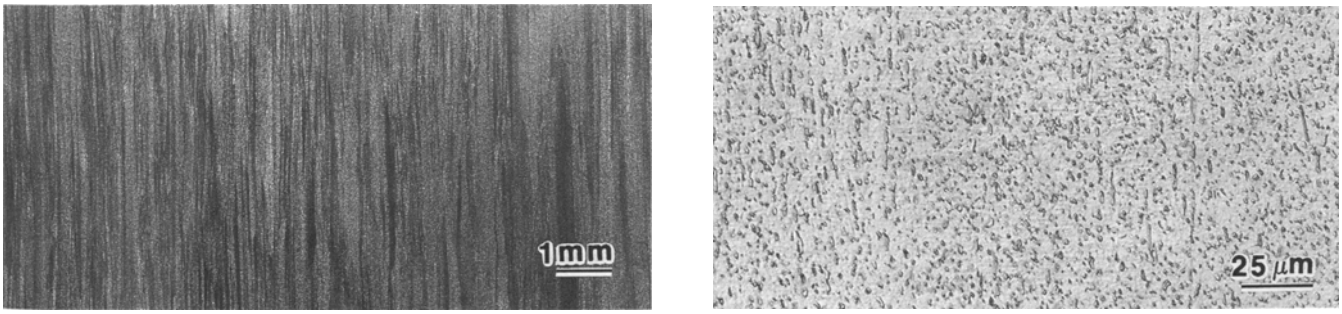

(a) (b)

Fig. 10 Morphology of the as-received LCB alloy. (a) Macrograph showing flow lines along prior deformation direction. (b) Micrograph showing α-phase particles distributed in the β-phase matrix along flow lines

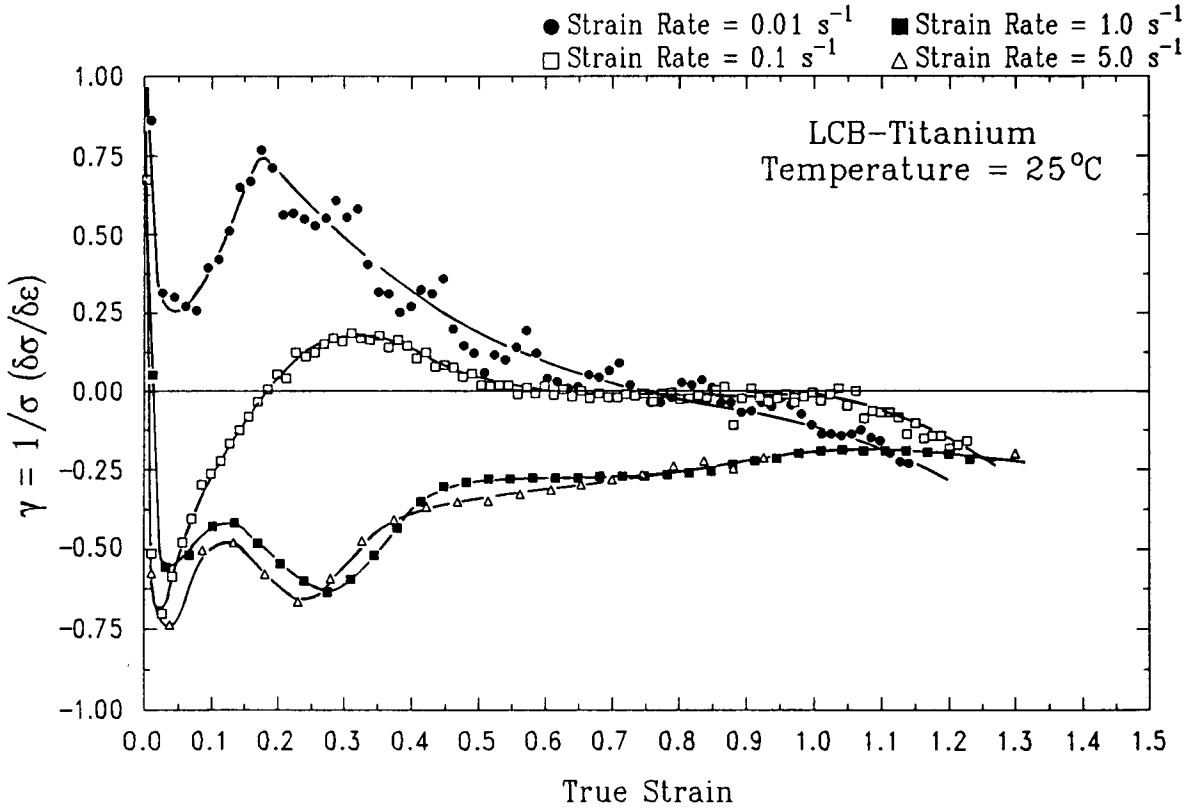

Fig. 11 Variation of the normalized work-hardening parameters, $\gamma = ([1/\sigma][\delta\sigma/\delta\varepsilon])$, for LCB alloy as a function of strain at different strain rates for room-temperature tests

microstructure consisted of equiaxed β grains, 50 to 200 μm in size (Fig. 1b). Figure 15 is a transmission electron micrograph (TEM) of a β grain with athermal ω-phase particles. The presence of the ω phase is evident from the extra spots and streaking in the diffraction pattern of $[110]_\beta$ orientation (Fig. 15b). At elevated temperatures, a large number of interstitials and vacancies are present in the structure. Upon rapid cooling, they cluster to form dislocation loops, as shown in Fig. 15(a). Some of the dislocation loops are partially open and appear as helical or curved dislocations. A few widely spaced slip lines are also revealed, which are probably caused by thermal stresses during cooling.

The ω phase is a nonequilibrium phase that can form either athermally during quenching from high temperature via a diffusionless process or isothermally by a diffusional process during moderate temperature (<400 °C, or 750 °F) aging. The presence of athermal ω phase does not have a pronounced effect on the mechanical properties of as-quenched β-titanium alloys (Ref 13). However, the ω phase affects the phase stability, microstructure, and mechanical properties of the material during the thermal or thermomechanical treatments that usually follow the quenching (Ref 14).

4.3.2 Microstructure during Cold Deformation at a Strain Rate of 0.01/s

Material deformed at room temperature at a strain rate of 0.01/s was examined after deformation to plastic strains of 0.06, 0.18, and 1.15. Optical micrographs revealing the progress of deformation during compression are shown in Fig. 16(a) to (c). Initially, the deformation is predominantly by single slip, with a small number of grains showing multiple slip (Fig. 16a). Further deformation to a strain of 0.18 leads to multiple slip in most grains (Fig. 16b). At very large strains of 1.15, the deformation is nonuniform due to the formation of dead metal zones. This results in a wavy pattern in the deformed grains (Fig. 16c). At a strain of 0.06, TEM examination reveals dislocations on a few parallel slip planes, as shown in Fig. 17. A few closed and partially open dislocation loops are also observed. Figure 18 shows that in grains that have undergone multiple slip, the slip bands have finer secondary slip lines. When the material is deformed to a higher strain of 0.18, the majority of the grains deform by multiple slip, as shown in Fig. 19. All the diffraction patterns (Fig. 17b, 18b, and 19b) show extra spots and streaking, indicating the presence of ω phase in the material.

The as-received LCB material shows a strong morphological texture, with the α-phase particles strung out in the direction of prior deformation (Fig. 10). Although solution treating above the transus temperature and fast cooling results in a structure of all β phase, the aligned grain morphology is still present and can be see even in material deformed to a strain of 0.06 (Fig. 12a). The morphological texture can cause anisotropic deformation behavior and can affect the resultant flow curves for the material. Deformation of metastable β-titanium alloys occurs by three different mechanisms: dislocation glide, twinning, and strain-induced

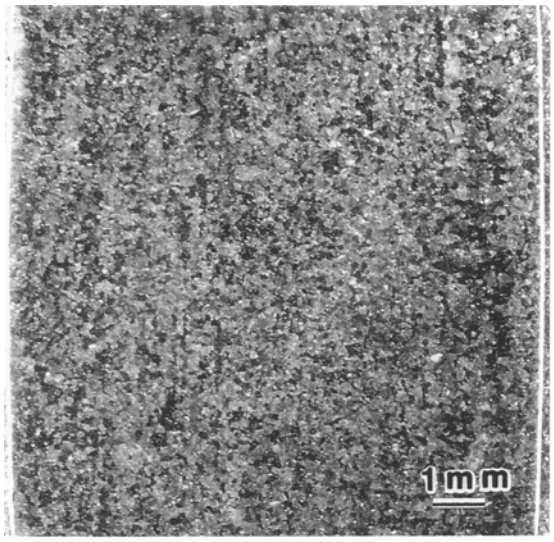

(a)

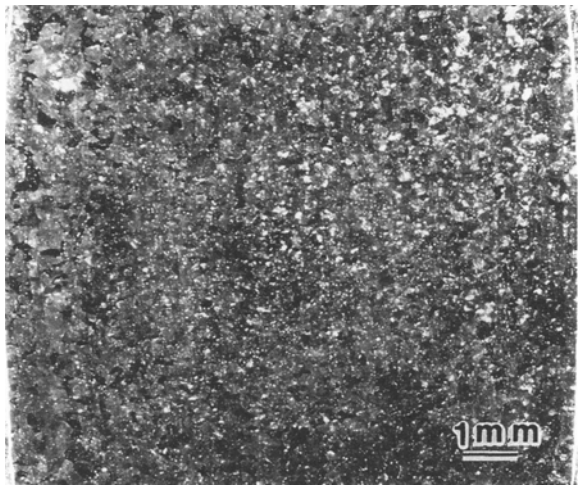

(b)

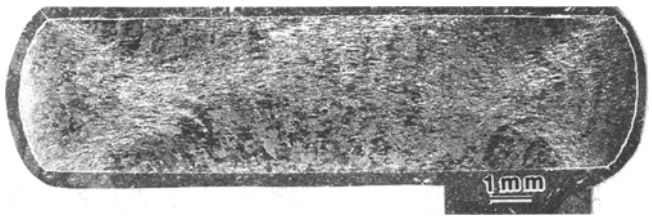

(c)

Fig. 12 Macrographs of specimens deformed at room temperature at a strain rate of 0.01/s to strains of 0.06 (a), 0.18 (b), and 1.15 (c)

martensitic transformation. Deformation by dislocation glide is characterized by a monotonic hardening behavior in the stress-strain curves (Ref 15). When the deformation occurs by {332} twinning, abrupt load drops occur during straining (Ref 15). The occurrence of strain-induced martensite causes abrupt changes in the work-hardening rate during deformation (Ref 13). The flow curve for deformation at a strain rate of 0.01/s,

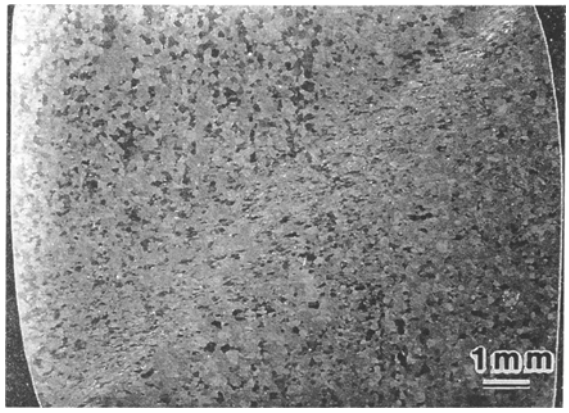

(a)

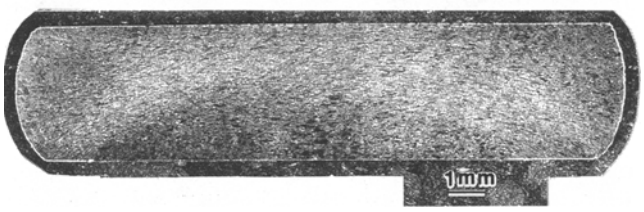

(b)

Fig. 13 Macrographs of specimens deformed at room temperature at a strain rate of 1/s to strains of 0.26 (a) and 1.3 (b)

shown in Fig. 4, indicated that the LCB material work hardens continuously, as is typical of the deformation by dislocation glide. Examination by TEM has shown the occurrence of slip as the primary mode of deformation, while {332} twinning was not observed in any of the specimens tested.

During the slip-dominated deformation of a bcc material, dislocation glide is usually observed in ⟨111⟩ directions. This is consistent with the TEM examination of the deformed LCB material. Differences in orientation of the four ⟨111⟩ slip directions can lead to single slip in some grains and multiple slip in others, as seen in Fig. 17 and 18 for deformation to a strain of 0.06. This type of slip has also been observed by others in Ti-15Mo-5Zr (Ref 16) and Ti-40V (Ref 17) alloys deformed under tension.

At a higher strain value of 0.18, a decrease in the relative intensity of the reflections from ω phase was observed (Fig. 19b). At yet a higher strain of 1.15, the reflections from the ω phase were not observed; the ω phase apparently disappears from the structure. Although these observations have not been quantified in this paper, this effect of cold deformation on the ω phase in the LCB alloy is particularly interesting and will be reported in a future publication (Ref 18). The volume fraction of the ω phase in the β-titanium alloys has been shown to either increase (Ref 19, 20) or decrease (Ref 21, 22) with deformation. A decrease in the volume fraction of ω phase with increasing plastic strain has also been observed in the β-phase alloy Timetal 21S (Ref 18). Like the 21S alloy, the LCB alloy investigated in the present study shows no precipitation of α during room-temperature deformation, despite an estimated increase in temperature of 200 °C (360 °F), as shown in Fig. 6.

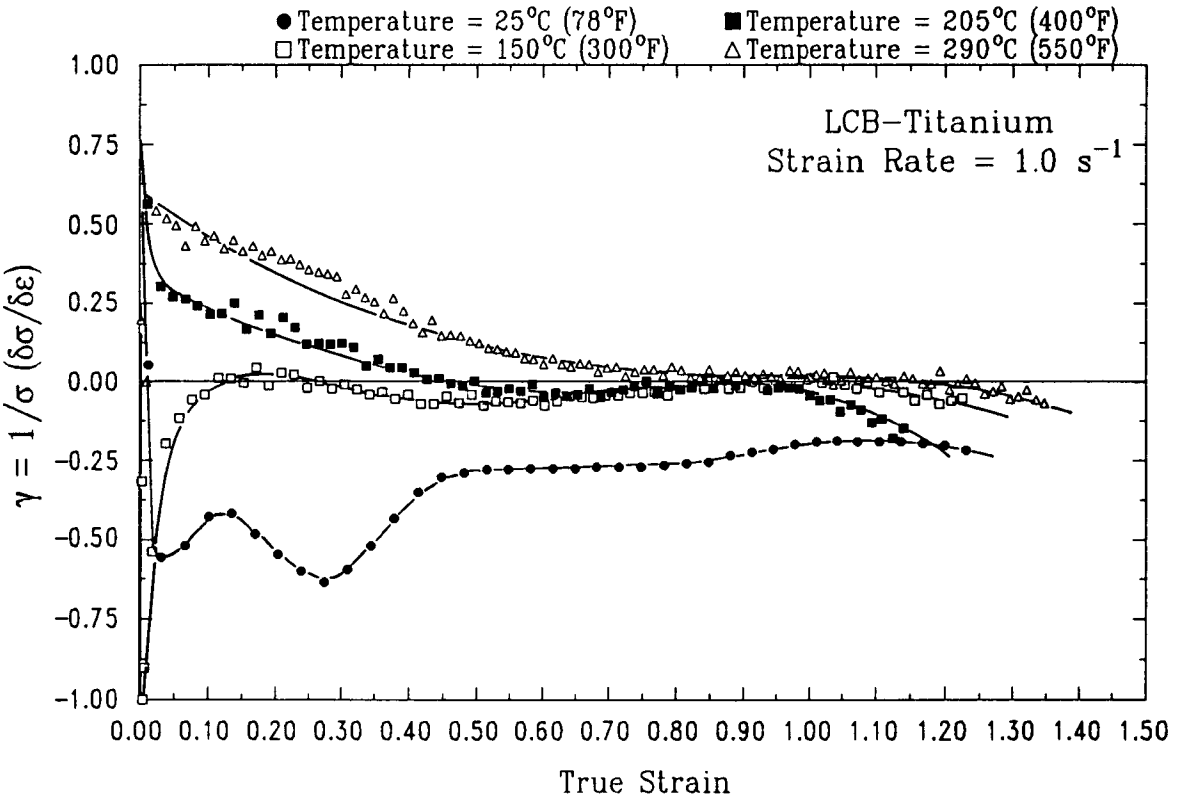

(a)

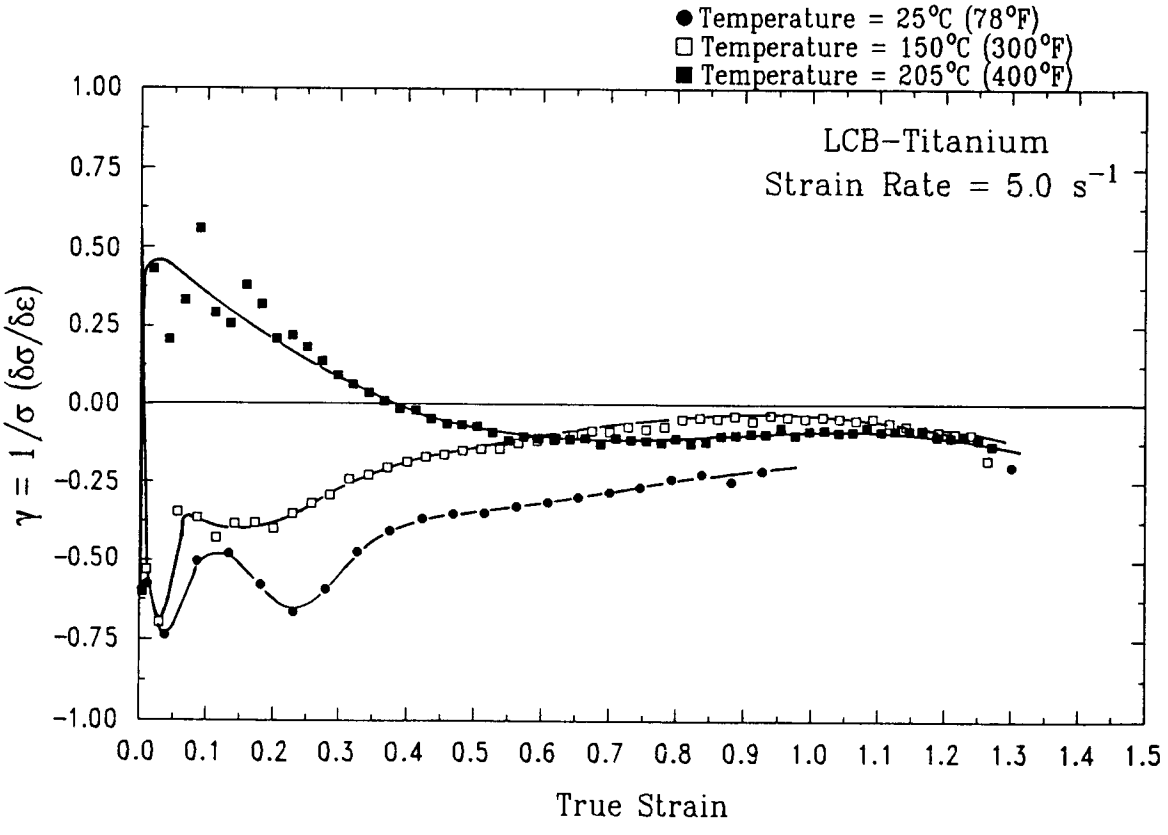

(b)

Fig. 14 Variation of the normalized work-hardening parameter, $\gamma = ([1/\sigma][\delta\sigma/\delta\varepsilon])$, for LCB alloy as a function of strain for warm tests at strain rates of 1/s (a) and 5/s (b)

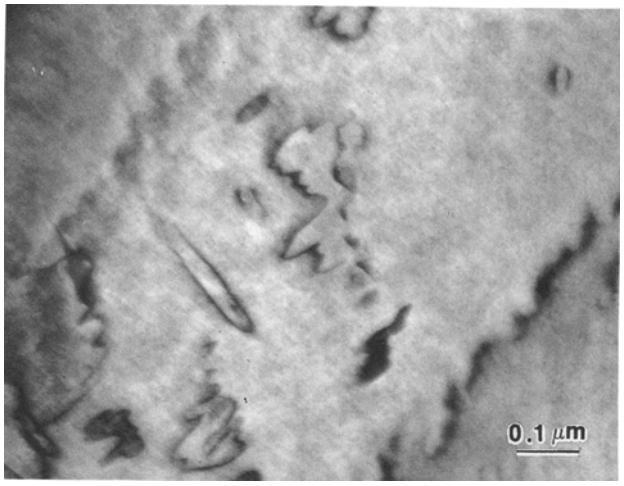

(a)

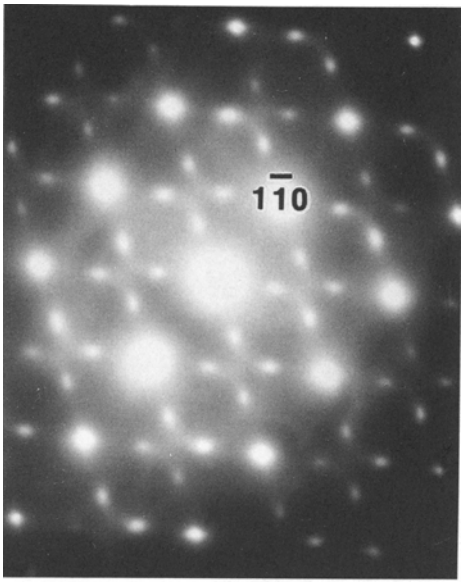

(b)

Fig. 15 (a) TEM micrograph of LCB alloy, solution heat treated at 815 °C (1500 °F) for 30 min and air cooled at 5 °C/s (9 °F/s). (b) Corresponding diffraction pattern, showing the presence of ω phase

(a)

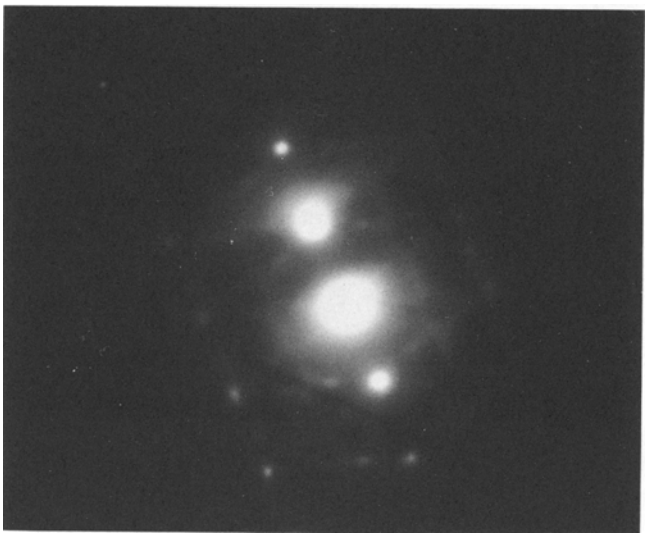

(b)

Fig. 17 (a) TEM micrograph of LCB alloy deformed to a strain of 0.06 at a strain rate of 0.01/s, showing single slip. (b) Corresponding diffraction pattern

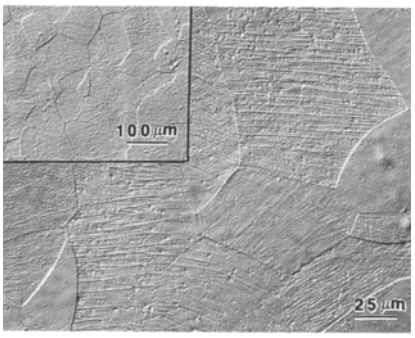

(a)

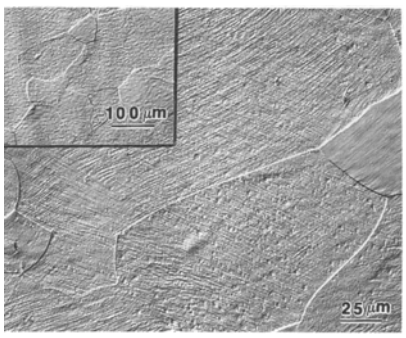

(b)

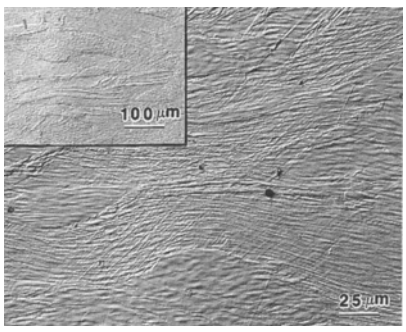

(c)

Fig. 16 Microstructure of LCB alloy deformed at a strain rate of 0.01/s to strains of 0.06 (a), 0.18 (b), and 1.15 (c)

4.3.3 Microstructure during Deformation at a Strain Rate of 0.1/s

Figure 20 shows an optical micrograph of the LCB alloy deformed at a rate of 0.1/s to a strain of 0.16. This strain corresponds to the minimum stress in the flow curve, beyond which the material work hardens. The microstructure shows the presence of multiple slip in the majority of β grains. Examination of the material by TEM confirms the occurrence of multiple slip in deformed β grains (Fig. 21). Some dislocation loops and curved dislocations similar to those seen in the as-received material were also observed. Like material deformed at a strain rate of 0.01/s, extra spots in the diffraction pattern, indicating the presence of ω phase, were also seen (Fig. 21b). Upon further deformation to a strain of 1.25, highly deformed β grains are observed (Fig. 22). As for slow-strain-rate deformation, although there was an estimated temperature rise of 350 °C (630 °F) (Fig. 6), precipitation of the α phase was not observed.

4.3.4 Microstructure during Deformation at a Strain Rate of 1.0/s

Deformation at a rate of 1.0/s results in inhomogeneous deformation. Optical macrographs reveal the presence of a shear band in a specimen deformed to a strain of 0.26 (Fig. 13a). The grains within the shear band are deformed to a high degree and appear elongated, whereas the grains outside the band appear to be equiaxed, as shown in Fig. 23(a) and (b), respectively. Slip

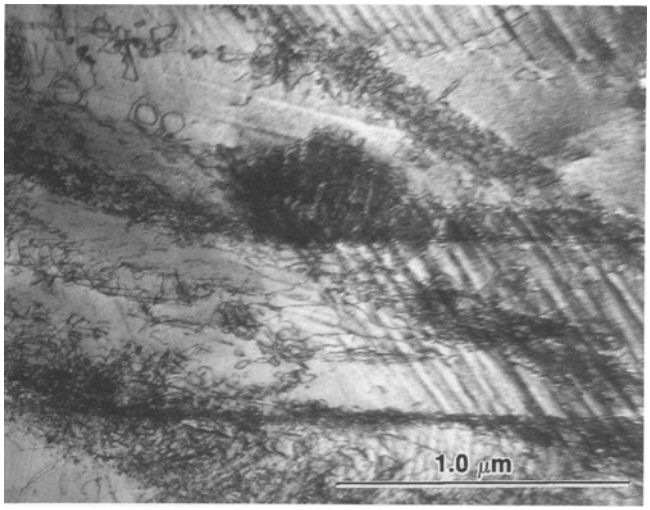

(a)

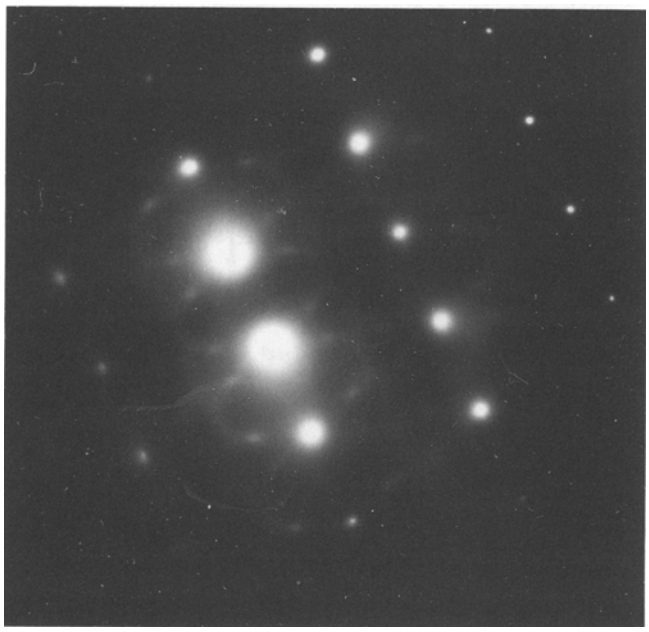

(b)

Fig. 18 (a) TEM micrograph of LCB alloy deformed to a strain of 0.06 at a strain rate of 0.01/s, showing multiple slip in a few grains. (b) Corresponding diffraction pattern

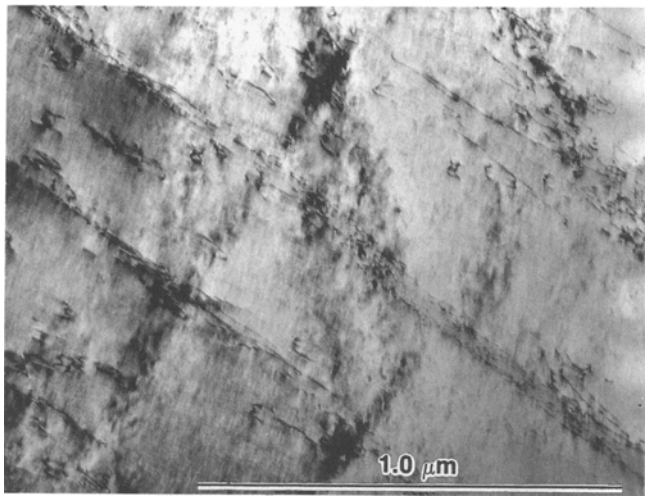

(a)

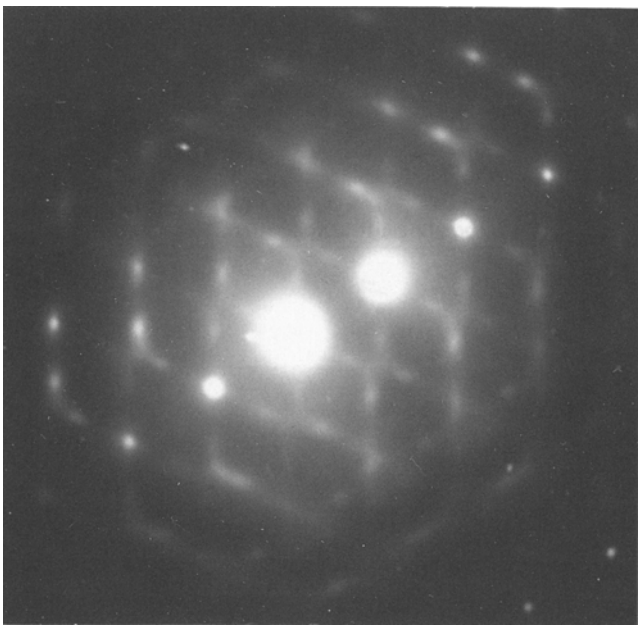

(b)

Fig. 19 (a) TEM micrograph of LCB alloy deformed to a strain of 0.18 at a strain rate of 0.01/s, showing multiple slip in all grains. (b) Corresponding diffraction pattern

lines are observed in some grains within the shear band. Specimens for TEM examination were taken from both within and outside the shear band. Examination reveals that outside the shear band, deformation is predominantly by planar slip, with some double slip (Fig. 24), whereas the areas within the shear band show multiple slip as the dominant mode of deformation (Fig. 25). Specimens deformed to a strain of 1.3 at a strain rate of 1/s show a macrostructure with inhomogeneous deformation and a pronounced shear band (Fig. 13b). The microstructure within the shear band consists of highly elongated β-phase grains that have undergone multiple slip (Fig. 26). Again, although the temperature increased considerably due to deformation heating (Fig. 6), precipitation of the α phase was not observed.

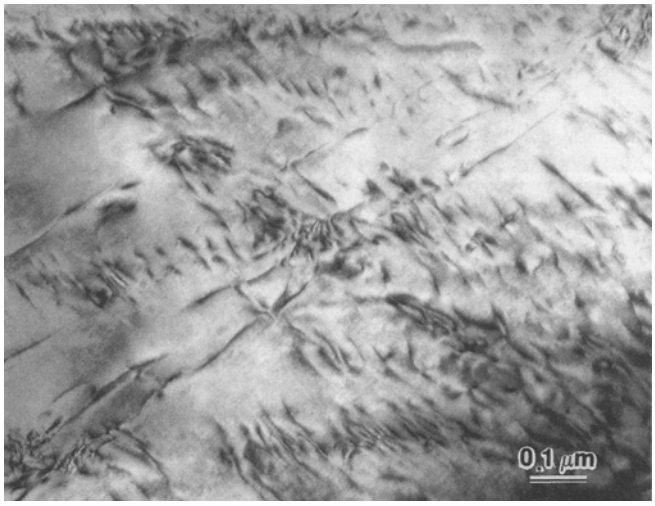

(a)

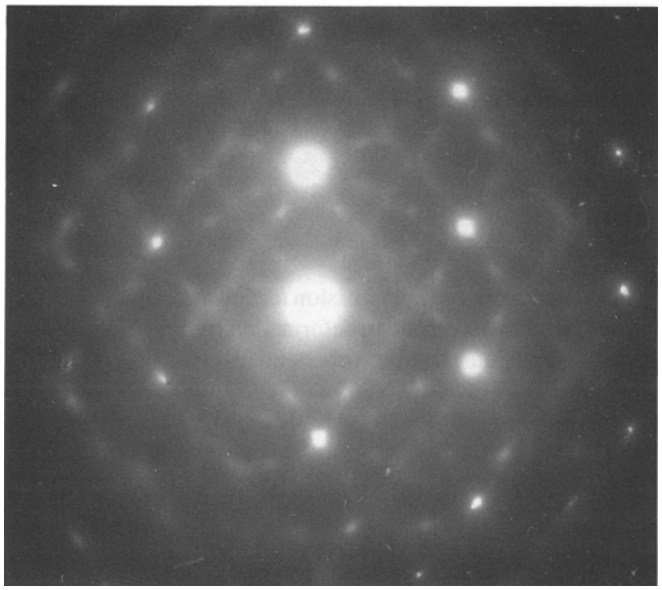

(b)

Fig. 21 (a) TEM micrograph of LCB alloy deformed to a strain of 0.16 at a strain rate of 0.1/s, showing multiple slip in all grains. (b) Corresponding diffraction pattern

5. Summary and Conclusions

The as-received Timetal LCB alloy, which had been annealed below the transus temperature, has a morphologically textured microstructure consisting of α particles distributed along the deformation direction in a matrix of β phase. Annealing for 30 min at a temperature of 815 °C (1500 °F), which is above the β-transus temperature, and cooling at 5 °C/s (9 °F/s) result in a single-phase β structure. Although the grains are recrystallized, the morphological texture persists in the single-phase material after annealing. Consequently, compression specimens with an aspect ratio of 1.5 tend to be mechanically unstable and fail by shear along planes inclined at 45° to the loading axis. When the aspect ratio is reduced to 1.125, the supertransus annealed material can be deformed at room tem-

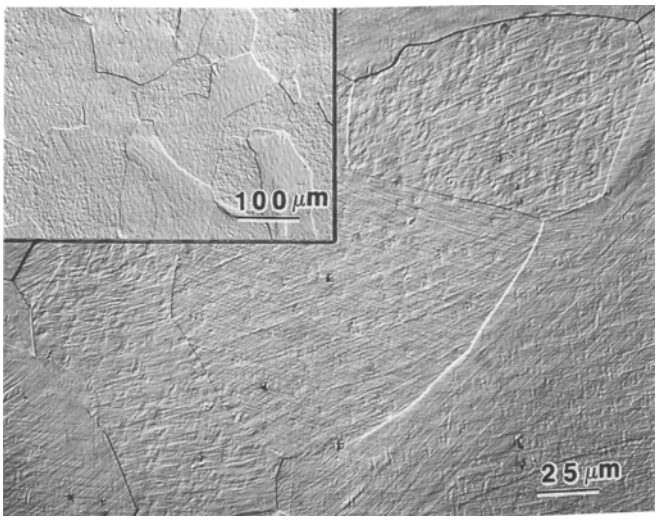

Fig. 20 Microstructure of a specimen of LCB alloy deformed at a strain rate of 0.1/s to a strain of 0.16, showing multiple slip in most grains

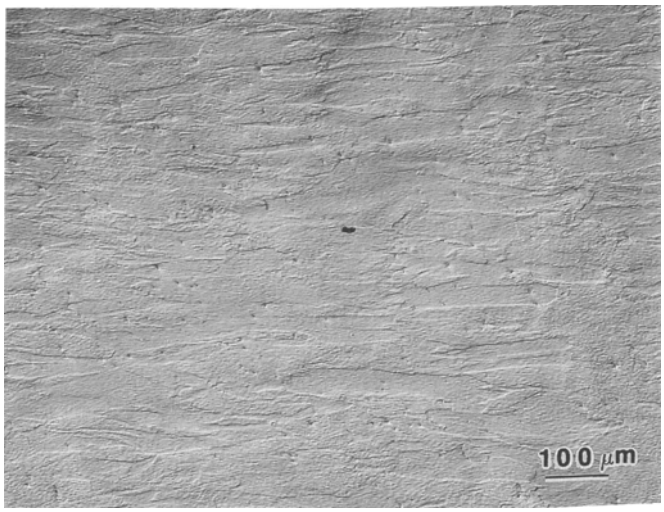

Fig. 22 Microstructure of a specimen of LCB alloy deformed at a strain rate of 0.1/s to a strain of 1.25, showing highly deformed β grains

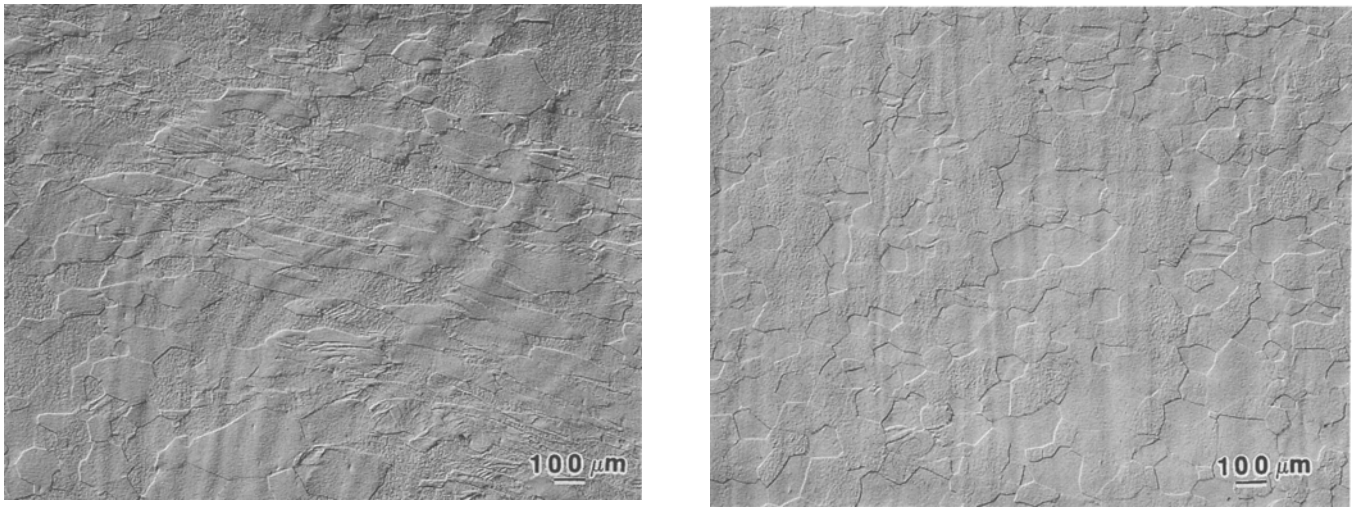

(a) (b)

Fig. 23 (a) Microstructures showing the appearance of grains in a specimen deformed to a strain of 0.26 at a strain rate of 1/s. (a) Elongated grains within the shear band. (b) Equiaxed grains outside the shear band

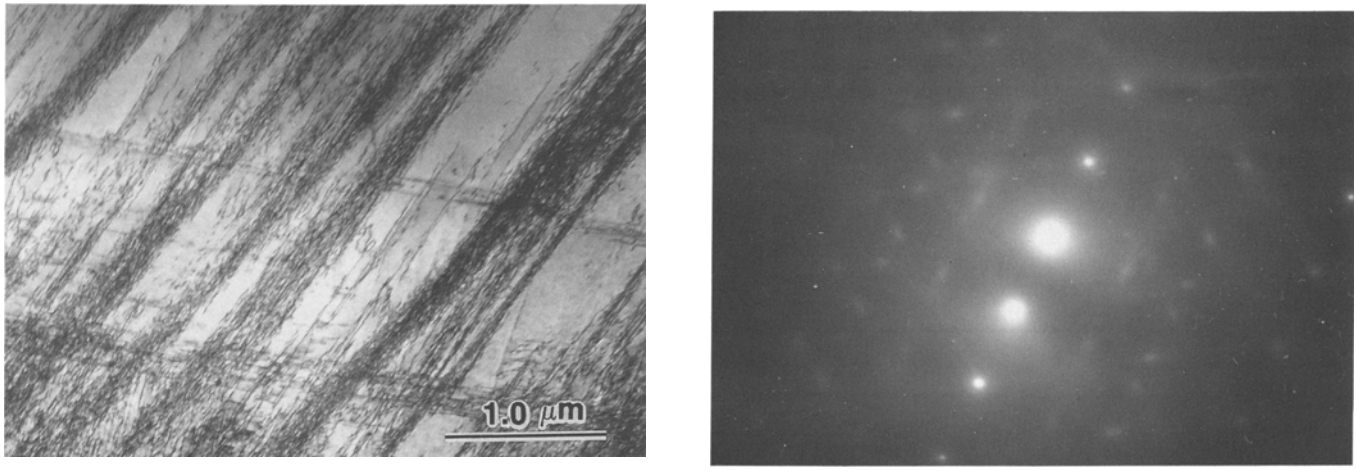

(a) (b)

Fig. 24 (a) TEM micrograph of LCB alloy deformed to an average strain of 0.26 at a strain rate of 1/s, showing planar slip in most grains outside the shear band. (b) Corresponding diffraction pattern

perature up to 75% reduction in height at strain rates ranging from 0.01 to 5/s. The as-received material fails by shear under the same deformation conditions. Aspect ratio and microstructure (phases present, as well as size, shape, and orientation of grains) are thus critical to the success of cold compressive forming of the LCB alloy.

Deformation at a slow strain rate (0.01/s) is characterized by work hardening, whereas flow softening occurs at fast strain rates (1 and 5/s). At an intermediate strain rate of 0.1/s, following a drop in stress after yielding, little work hardening is observed, and plastic deformation occurs at almost constant flow stress. At all strain rates, deformation initially occurs by single slip in most grains, which changes to multiple slip after a strain of approximately 0.15. Associated with the change in slip behavior is an increase in the work-hardening rate. At slow strain rates of 0.01 and 0.1/s, the increased work hardening leads to stable deformation. However, at strain rates of 1 and 5/s, localized deformation in the form of shear bands leads to continuous flow softening.

Room-temperature compression testing at strain rates in the range of 0.01 to 5/s results in deformation heating of the specimens, which in turn results in an estimated temperature rise in the range of 200 to 500 °C (360 to 900 °F) after deformation to strains in the range of 1.15 to 1.30. Despite this large rise in temperature, no precipitation of the α phase was observed in the metastable β-titanium alloy.

If the initial temperature of the specimen is increased to between 150 and 250 °C (300 and 480 °F), stable deformation associated with work hardening is observed at strain rates of 1 and 5/s. This is of considerable industrial significance because most forming operations result in strain rates of 1/s or greater in the workpiece.

The nature of plastic deformation changes considerably with strain in the LCB alloy. At all strain rates, the initial stages

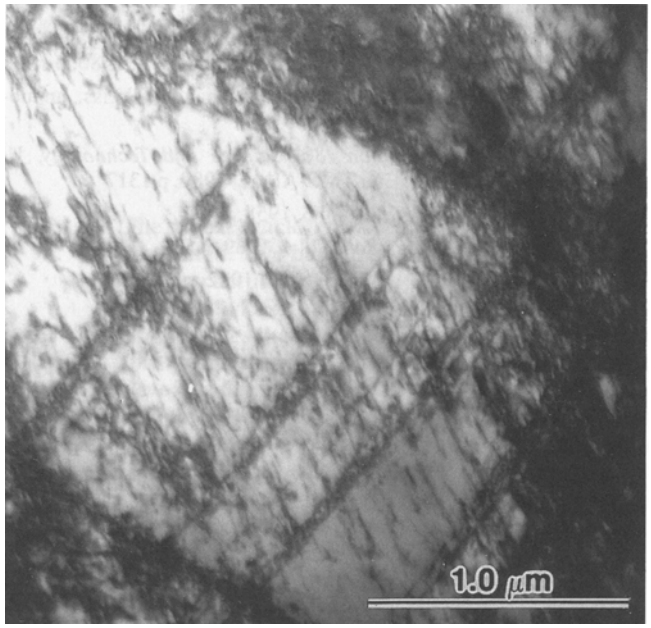

(a)

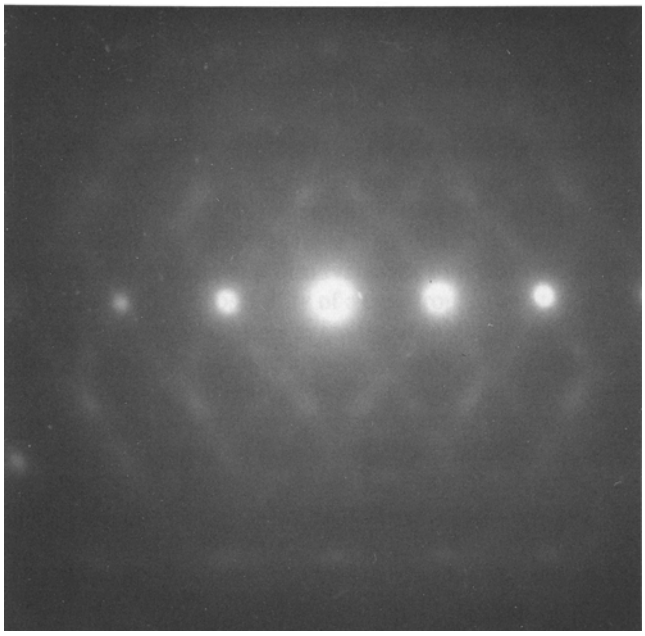

(b)

Fig. 25 (a) TEM micrograph of LCB alloy deformed to an average strain of 0.26 at a strain rate of 1/s, showing multiple slip in grains within the shear band. (b) Corresponding diffraction pattern

of deformation show clear, well-defined slip lines, which are replaced at higher strains by multiple slip, resulting in an increased work-hardening rate. In general, the work-hardening rate may decrease at high strains if the dislocations are able to cross-slip or climb, provided there is sufficient thermal activation. This would result in a change of slip character from planar to wavy glide. At small strains, temperature rise in the specimens due to deformation heating may not provide the necessary thermal activation. However, at larger strains, the estimated temperature rise of 200 to 500 °C (360 to 900 °F) at strain rates of ≥0.1/s may activate cross-slip within the shear bands.

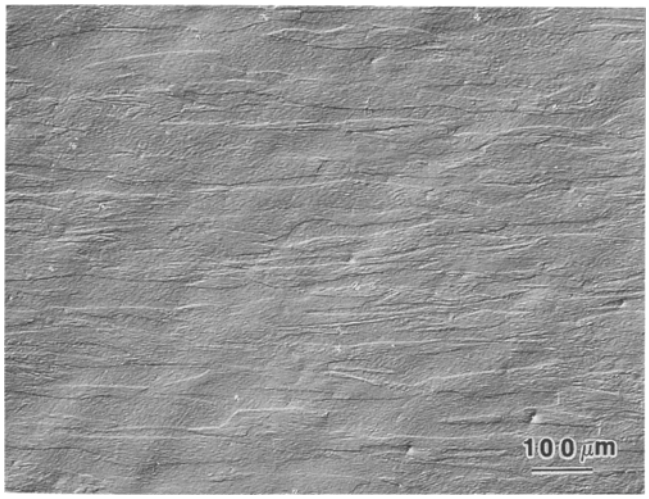

Fig. 26 Microstructure of a specimen of LCB alloy deformed at a strain rate of 1/s to a strain of 1.3, showing highly deformed β grains

Acknowledgments

Support of this work by the U.S. Air Force Wright Laboratory—Materials Directorate is acknowledged. The authors would also like to thank Drs. Paul Bania and Paul Allen of TIMET for stimulating discussions during the course of this work.

References

1. P.J. Bania, in *Beta Titanium Alloys in the 1990s,* D. Eylon, R.R. Boyer, and D.A. Koss, Ed., Minerals, Metals & Materials Society, 1993, p 3-14
2. A.M. Sherman and J.E. Allison, SAE Technical Paper No. 860608, Society of Automotive Engineers, 1986
3. P.A. Blankinsop, in *Titanium Science and Technology,* G. Luetjering, U. Zwicker, and W. Bunk, Ed., DGM Publishers, Oberursel, FRG, 1985, p 2323-2338
4. P.G. Allen and A.J. Hutt, in *Proceedings of the 1994 International Titanium Conference,* Titanium Development Association, 1994, p 397
5. "Low-Cost Beta Titanium," journal announcement, *Mech. Eng.,* July 1993, p 64
6. P. Dadras and J.F. Thomas, Jr., *Metall. Trans. A,* Vol 12A, 1981, p 1867
7. P.W. Lee and H.A. Kuhn, in *Workability Testing,* American Society for Metals, 1984, p 37-50
8. A.T. Male and G.E. Dieter, in *Workability Testing,* American Society for Metals, 1984, p 51-72
9. L.W. Meyer and E. Staskewitsch, in *Titanium '92 Science and Technology,* F.H. Froes and I. Caplan, Ed., TMS-AIME, 1993, p 1939-1946
10. D.K. Matlock, F. Zia-Ebrahimi, and G. Krauss, *Deformation, Processing and Structure,* American Society for Metals, 1984 p 47-87

11. S.L. Semiatin and G. Lahoti, *Metall. Trans. A*, Vol 13A, 1981, p 1705
12. S.L. Semiatin and G. Lahoti, *Metall. Trans. A*, Vol 12A, 1982, p 275
13. T.W. Duering and J.C. Williams, in *Beta Titanium Alloys in the 1980s*, R.R. Boyer and H.W. Rosenberg, Ed., TMS-AIME, 1984, p 24-61
14. A.W. Bowen, in *Beta Titanium Alloys in the 1980s*, R.R. Boyer and H.W. Rosenberg, Ed., TMS-AIME, 1984, p 85-106
15. O. Izumi, in *Titanium '80, Science and Technology*, H. Kimura and O. Izumi, Ed., TMS-AIME, 1980, p 133-139
16. S. Hanada and O. Izumi, *Metall. Trans. A*, Vol 6A, 1975, p 1737
17. D.A. Koss and J.C. Chesnutt, in *Titanium '80, Science and Technology*, H. Kimura and O. Izumi, Ed., TMS-AIME, 1980, p 1097
18. M. Saqib, N. Stefansson, R. Srinivasan, and I. Weiss, unpublished work, 1995
19. A.W. Bowen, in *Titanium '80, Science and Technology*, H. Kimura and O. Izumi, Ed., TMS-AIME, 1980, p 1317
20. J.M. Silcock, *Acta Metall.*, Vol 6, 1958, p 481
21. B.S. Hickman, *J. Mater. Sci.*, Vol 4, 1969, p 554
22. S.K. Sikka, *Prog. Mater. Sci.*, Vol 27, 1982, p 245